LIPUS-mediated mechanotransduction activates the YAP/TAZ/SCX axis and enhances tenogenesis-associated responses in tendon stem cells

SHANGBIN LI[1], YANG HU[1], KAILUN ZHENG[1], LIXIN CHEN[1], DIJUN LI[2] and YUN LI[1]

[1]Department of Rehabilitation Medicine, The Third Clinical Medical College of China Three Gorges University, Gezhouba Central Hospital of Sinopharm, Yichang, Hubei 443000, P.R. China; [2]Department of Orthopedics, The Second Hospital of Shanxi Medical University, Taiyuan, Shanxi 030001, P.R. China

Received May 27, 2026; Accepted August 7, 2026

DOI: 10.3892/br.2026.2199

Abstract. Tendon healing is frequently accompanied by fibrosis, scar formation and incomplete functional recovery. Tendon stem cells (TSCs) are central to tendon regeneration; however, the molecular basis by which low-intensity pulsed ultrasound (LIPUS) regulates their tenogenesis-associated behavior through mechanotransduction remains incompletely understood. In the present study, it was investigated whether LIPUS enhances tenogenesis-associated responses and matrix-related gene expression in rat TSCs through the YAP/TAZ/SCX signaling axis. Public transcriptomic data from the Gene Expression Omnibus database (GSE273466) were analyzed to identify differentially expressed genes and enriched pathways associated with LIPUS exposure. Primary rat Achilles tendon-derived TSCs were isolated, expanded and characterized by morphology and flow cytometry. Passage-3 TSCs were assigned to the Control, LIPUS and LIPUS + Verteporfin (VP) groups. Cell migratory behavior was evaluated using a scratch assay. Immunofluorescence staining, western blotting and reverse transcription-quantitative PCR were performed to assess the expression of YAP, TAZ, SCX, COL I and TNMD. Transcriptomic analysis indicated that LIPUS enriched mechanotransduction-related, cytoskeleton-associated, and YAP/TAZ-related signaling programs, together with enhanced SCX-associated signatures. Cultured cells exhibited a typical TSC phenotype, characterized by positive expression of CD90, CD105 and CD146 and negative expression of CD11b, CD34 and CD45. LIPUS increased scratch closure at 24 and 48 h and upregulated YAP, TAZ, SCX, COL I and TNMD at the protein and/or mRNA level. These effects were attenuated by VP treatment. In conclusion, LIPUS enhances a tenogenesis-associated molecular phenotype in TSCs and promotes matrix-related gene expression, at least in part through mechanotransduction-dependent activation of YAP/TAZ signaling and upregulation of SCX. These findings provide mechanistic support for further investigation of LIPUS as a strategy for tendon regeneration.

Correspondence to: Dr Yun Li, Department of Rehabilitation Medicine, Sinopharm Gezhouba Central Hospital, 60 Xiling 1st Road, Xiling, Yichang, Hubei 443000, P.R. China
E-mail: 1427510435@qq.com

Key words: low-intensity pulsed ultrasound, tendon stem cells, YAP/TAZ, scleraxis, mechanotransduction, tendon regeneration

Introduction

Tendon injury is a common musculoskeletal disorder that frequently causes pain, functional limitation and long-term impairment in quality of life (1,2). Because tendon tissue is relatively hypocellular and hypovascular, its intrinsic regenerative capacity is limited, and healing often culminates in fibrosis, inferior mechanical performance and an increased risk of re-injury (3,4). Although current therapeutic strategies, including surgical repair, biomaterial-based approaches and cell-based interventions, may improve structural restoration, complete functional regeneration remains difficult to achieve (5-7). Accordingly, there is a clear need to identify biological strategies that can more effectively promote tendon repair.

The mechanical microenvironment is now recognized as a major determinant of stem cell behavior and lineage commitment (8,9). Mechanical cues regulate proliferation, migration and differentiation through mechanotransduction pathways involving integrins, cytoskeletal remodeling, Rho GTPases, and transcriptional coactivators such as Yes-associated protein (YAP) and transcriptional coactivator with PDZ-binding motif (TAZ) (10-14). In tendon biology, scleraxis (SCX) is a canonical transcription factor required for tendon development and maintenance of the tenogenic program (15,16). The YAP/TAZ-SCX axis therefore represents a plausible molecular interface through which external mechanical stimulation may influence tenogenesis-associated cell fate decisions.

Low-intensity pulsed ultrasound (LIPUS) is a noninvasive biophysical intervention with documented regenerative and anti-inflammatory effects (17,18). By delivering acoustic mechanical energy to cells and tissues, LIPUS can modulate mechanosensitive signaling and alter cellular behavior (19,20). Previous studies have suggested that LIPUS may facilitate tendon and tendon-bone healing (21,22); however, the molecular events linking LIPUS-derived mechanical stimulation

to TSC fate remain insufficiently defined, particularly with respect to YAP/TAZ- and SCX-associated signaling.

In the present study, transcriptomic analysis was combined with *in vitro* experiments to examine whether LIPUS activates mechanotransduction-related pathways in rat TSCs and thereby enhances YAP/TAZ- and SCX-associated responses. It was hypothesized that LIPUS would induce a tenogenesis-associated molecular program characterized by increased YAP/TAZ signaling, upregulation of SCX, and enhanced expression of matrix-related markers.

Materials and methods

Primary cell source. Two specific pathogen-free male Sprague-Dawley rats, aged 3-4 weeks and weighing 80-100 g, were used exclusively for primary tendon stem cell (TSC) isolation. The animals were maintained under standard laboratory conditions, including a controlled temperature of 20-26˚C, relative humidity of 40-70%, and a 12/12-h light/dark cycle. Food and sterile drinking water were provided *ad libitum* throughout the experimental period. All subsequent experiments were performed using expanded *in vitro* cell passages derived from these primary cultures and were repeated independently. The animals were obtained from the Experimental Animal Center of Shanxi Medical University. The present study was approved by the Animal Welfare Ethics Committee of the Second Hospital of Shanxi Medical University (approval no. DW20230008; Taiyuan, China), and all procedures were conducted in accordance with institutional and national guidelines for animal care and use. At the end of tissue collection, rats were euthanized by intraperitoneal injection of an overdose of sodium pentobarbital (200 mg/kg). Death was confirmed by the absence of spontaneous respiration, heartbeat, and pedal withdrawal reflex before tendon harvest.

Main reagents and instruments. The major reagents used in the present study were PBS (cat. no. P7209; LABLEAD), penicillin-streptomycin (cat. no. 15140122; Thermo Fisher Scientific, Inc.), serum-free cryopreservation solution (cat. no. 12648010; Thermo Fisher Scientific, Inc.), collagenase type I (cat. no. 17100017; Thermo Fisher Scientific, Inc.), RIPA lysis buffer (cat. no. 89901; Thermo Fisher Scientific, Inc.), protease inhibitor cocktail (cat. no. 78429; Thermo Fisher Scientific, Inc.), TRIzol reagent (cat. no. 15596026CN; Thermo Fisher Scientific, Inc.), reverse transcription kit (cat. no. 4366596; Thermo Fisher Scientific, Inc.), SYBR Green qPCR mix (cat. no. K0223; Thermo Fisher Scientific, Inc.), BCA protein assay kit (cat. no. 23227; Thermo Fisher Scientific, Inc.), 0.25% trypsin-EDTA (cat. no. 25200056; Gibco; Thermo Fisher Scientific, Inc.), α-MEM (cat. no. 12571063; Gibco; Thermo Fisher Scientific, Inc.), fetal bovine serum (cat. no. 10099141C; Thermo Fisher Scientific, Inc.), PVDF membranes (cat. no. IPVH00010) and Verteporfin (VP; cat. no. HY-B0146; CL 318952; MedChemExpress).

Primary antibodies used for western blotting and immunofluorescence were all purchased from Abcam, including anti-YAP (cat. no. ab52771), anti-TAZ (cat. no. ab84927), anti-SCX (cat. no. ab58655), anti-COL I (cat. no. ab34710) and anti-β-actin (cat. no. ab8226). Antibodies used for flow cytometry were purchased from Thermo Fisher Scientific, Inc., including CD90 (cat. no. A15761), CD105 (cat. no. 12-1057-42), CD146 (cat. no. 11-1469-42), CD11b (cat. no. 12-0112-82), CD34 (cat. no. 48-0341-82) and CD45 (cat. no. MHCD4530). Corresponding horseradish peroxidase-conjugated and fluorescent secondary antibodies (cat. no. ab6721) were obtained from Abcam.

The principal instruments included a humidified CO_2 incubator (Thermo Fisher Scientific, Inc.), an inverted fluorescence microscope (Leica Microsystems GmbH), a real-time PCR system (Bio-Rad Laboratories, Inc.), a microplate reader (BioTek; Agilent Technologies, Inc.), a biosafety cabinet (Shanghai Lishen), a high-speed centrifuge (Eppendorf SE), a flow cytometer (Beckman Coulter, Inc.), and a LIPUS device (Welld).

Isolation and culture of TSCs. Achilles tendons were harvested aseptically, minced into fragments of ~1 mm, and digested with collagenase type I at 37˚C for 1 h with gentle agitation. After centrifugation at 300 x g for 5 min at room temperature, the cell suspension was seeded into culture dishes containing α-MEM supplemented with 10% fetal bovine serum and 1% penicillin-streptomycin and maintained at 37˚C in a humidified atmosphere of 5% CO_2. During primary culture, non-adherent cells were removed by repeated medium replacement, which allowed enrichment of the adherent TSC population. The adherent cells were expanded by routine passaging when cultures reached 80-90% confluence. Cells were passaged at a ratio of 1:3, and passage-3 TSCs were used for all subsequent experiments. All experiments were independently repeated at least three times using independently prepared cultures derived from the same primary TSC isolation.

Flow cytometric identification of TSCs. Passage-3 TSCs were dissociated with 0.25% trypsin-EDTA, washed three times with PBS, and resuspended as single-cell suspensions at a final concentration of ~$1x10^6$ cells/ml. Cells were incubated with fluorophore-conjugated antibodies against CD90 (1:100), CD105 (1:100), CD146 (1:100), CD11b (1:100), CD34 (1:100) and CD45 (1:100) for 30 min at 4˚C in the dark, with matched isotype controls included for each channel. After washing, the cells were analyzed using a flow cytometer (FC500; Beckman Coulter, Inc.), and the data were processed using the corresponding acquisition software (FlowJo v10.8.1; FlowJo LLC). Cells positive for CD90, CD105 and CD146 and negative for CD11b, CD34 and CD45 were considered consistent with the TSC phenotype.

Experimental grouping and treatment. Passage-3 TSCs were assigned to three groups: Control, LIPUS and LIPUS + VP. Cells in the LIPUS group were exposed to LIPUS at a frequency of 1.5 MHz, an intensity of 50 mW/cm^2, a pulse repetition frequency of 1 kHz, a duty cycle of 20%. Cells received two treatment sessions of 25 min each, with a 24-h interval between sessions. Cells in the LIPUS + VP group were pretreated with VP at a final concentration of 1 μmol/l for 1 h before each LIPUS session. Control cells were cultured under identical conditions without LIPUS or VP treatment. All downstream assays were performed after the treatment period.

Although a VP-only group was not included, the concentration of VP (1 μmol/l) and the 1-h pretreatment duration were selected based on previously established protocols. The Control group was maintained under identical culture conditions without LIPUS or VP treatment.

Scratch-wound assay. TSCs were seeded in 6-well plates at $5x10^5$ cells/well and cultured until a confluent monolayer was formed. A linear scratch was created using a sterile 200-μl pipette tip, and detached cells were removed by washing with PBS. Cells were then maintained in basal medium, and images of the same wound area were acquired at 0, 24, and 48 h under an inverted microscope. Scratch closure was quantified using ImageJ software according to the following formula: wound closure (%)=[(initial wound area-residual wound area)/initial wound area x100%].

Western blotting. TSCs were seeded in 6-well plates at $2x10^5$ cells/well. After treatment, total cellular protein was extracted using RIPA lysis buffer supplemented with protease inhibitors. Protein concentration was determined using a BCA assay, and equal amounts of protein (20 μg per lane) were loaded per lane. Samples were separated on 10% SDS-PAGE gels and transferred onto PVDF membranes. After blocking with 5% non-fat milk for 2 h at room temperature, the membranes were incubated overnight at 4˚C with primary antibodies against YAP (1:1,000), TAZ (1:1,000), SCX (1:1,000), COL I (1:1,000) andβ-actin (1:5,000). After washing with TBST (containing 0.1% Tween-20), membranes were incubated with horseradish peroxidase-conjugated secondary antibodies (1:5,000) for 1 h at room temperature. Immunoreactive bands were visualized using enhanced chemiluminescence (cat. no. P0018AS; Beyotime Institute of Biotechnology) and quantified using ImageJ. Equal amounts of total protein were loaded in each lane, and β-actin was used as the loading control for normalization. The total β-actin signal showed no apparent difference among the experimental groups under the present LIPUS treatment conditions.

Reverse transcription-quantitative PCR (RT-qPCR). Total RNA was extracted from treated cells using TRIzol reagent according to the manufacturer's protocol. The thermocycling conditions were as follows: Initial denaturation at 95˚C for 30 sec, followed by 40 cycles of denaturation at 95˚C for 5 sec and annealing/extension at 60˚C for 30 sec; a melt-curve analysis was performed to confirm amplification specificity. Complementary DNA was synthesized using a reverse transcription kit, and quantitative PCR was performed using SYBR Green chemistry on a real-time PCR system. Reverse transcription was performed using the kit according to the manufacturer's instructions. The expression levels of target genes, including COL1A1 and TNMD were normalized to GAPDH, and relative mRNA expression was calculated using the $2^{-\Delta\Delta Cq}$ method (23). Each assay was performed using at least three independent biological replicates. The sequences of primers used in the present study are as follows: TNMD forward, 5'-GTGAAGGTGGAGAAGACCCG-3' and reverse, 5'-TTGCCTCGACGGCAGTAAAT-3'; COL1A1 forward, 5'-GTTTGGAGAGAGCATGACCGA-3' and reverse, 5'-ACAAGCGTGCTGTAGGTGAA-3'; and GAPDH forward, 5'-TCACTGCCACCCAGAAGAC-3' and reverse, 5'-TGTAGGCCATGAGGTCCAC-3'.

Immunofluorescence staining. TSCs were seeded in 6-well plates at $2x10^5$ cells/well and processed after treatment. Cells were fixed with 4% paraformaldehyde for 30 min, washed with PBS, permeabilized with 0.3% Triton X-100 for 5 min, and blocked with 5% goat serum (cat. no. BL1097A; Labgic) for 30 min at room temperature. The samples were then incubated overnight at 4˚C with primary antibodies against SCX (1:1,000) and COL I (1:1,000), followed by incubation with fluorescent secondary antibodies (1:100) for 1 h at room temperature in the dark. Nuclei were counterstained with DAPI (5 mg/ml; cat. no. C1002; Beyotime Institute of Biotechnology). Fluorescence images were acquired using identical exposure settings for all groups and quantified using ImageJ software (version 2.14.0; National Institutes of Health). For each sample, at least three representative fields were analyzed.

Transcriptomic analysis. Transcriptomic data were obtained from Gene Expression Omnibus (GEO; https://www.ncbi.nlm.nih.gov/geo/) (GSE273466) (24). Raw data underwent quality control and normalization. Differentially expressed genes between Control and LIPUS groups were identified using $|\log_2$ fold change$|>1$ and FDR <0.05. Gene Ontology (GO) enrichment analysis was performed to identify biological processes (BP), cellular components (CC) and molecular functions (MF) associated with LIPUS exposure. Gene set enrichment analysis (GSEA) evaluated YAP1- and SCX-associated signatures. Analyses were performed using Python-based workflows, including statsmodels, bioinfokit and gseapy.

Statistical analysis. Statistical analyses were performed using SPSS 21.0, and graphs were generated using GraphPad Prism 9.0 (Dotmatics). All experiments were repeated at least three times using independently prepared cultures. Data distribution was assessed using the Shapiro-Wilk test. For normally distributed data, comparisons between two groups were performed Transcriptomic data were obtained from GEO (GSE273466). Raw data underwent quality control and normalization. Differentially expressed genes between Control and LIPUS groups were identified using $|\log_2$ fold change$|>1$ and FDR <0.05. GO enrichment analysis was performed to identify BP, CC and MF associated with LIPUS exposure. GSEA evaluated YAP1- and SCX-associated signatures. Analyses were performed using Python-based workflows, including statsmodels (https://www.statsmodels.org/), bioinfokit (https://github.com/reneshbedre/bioinfokit) and gseapy (https://gseapy.readthedocs.io/). For normally distributed data, comparisons between two groups were performed using the unpaired two-tailed Student's t-test. For data that did not meet the assumptions of normality, the Mann-Whitney U test was applied. Data are presented as the mean ± SD. Unless otherwise stated, all experiments were repeated independently at least three times. $P<0.05$ was considered to indicate a statistically significant difference.

Results

LIPUS-induced transcriptomic alterations are associated with mechanotransduction and tenogenic differentiation. To investigate the molecular basis of the LIPUS response, the transcriptomic dataset GSE273466 was first analyzed. The heatmap and volcano plot revealed a distinct separation in gene expression patterns between the Control and LIPUS groups, indicating that LIPUS substantially altered the transcriptional landscape of TSCs (Fig. 1A and B). GO enrichment analysis further showed that the differentially expressed genes were

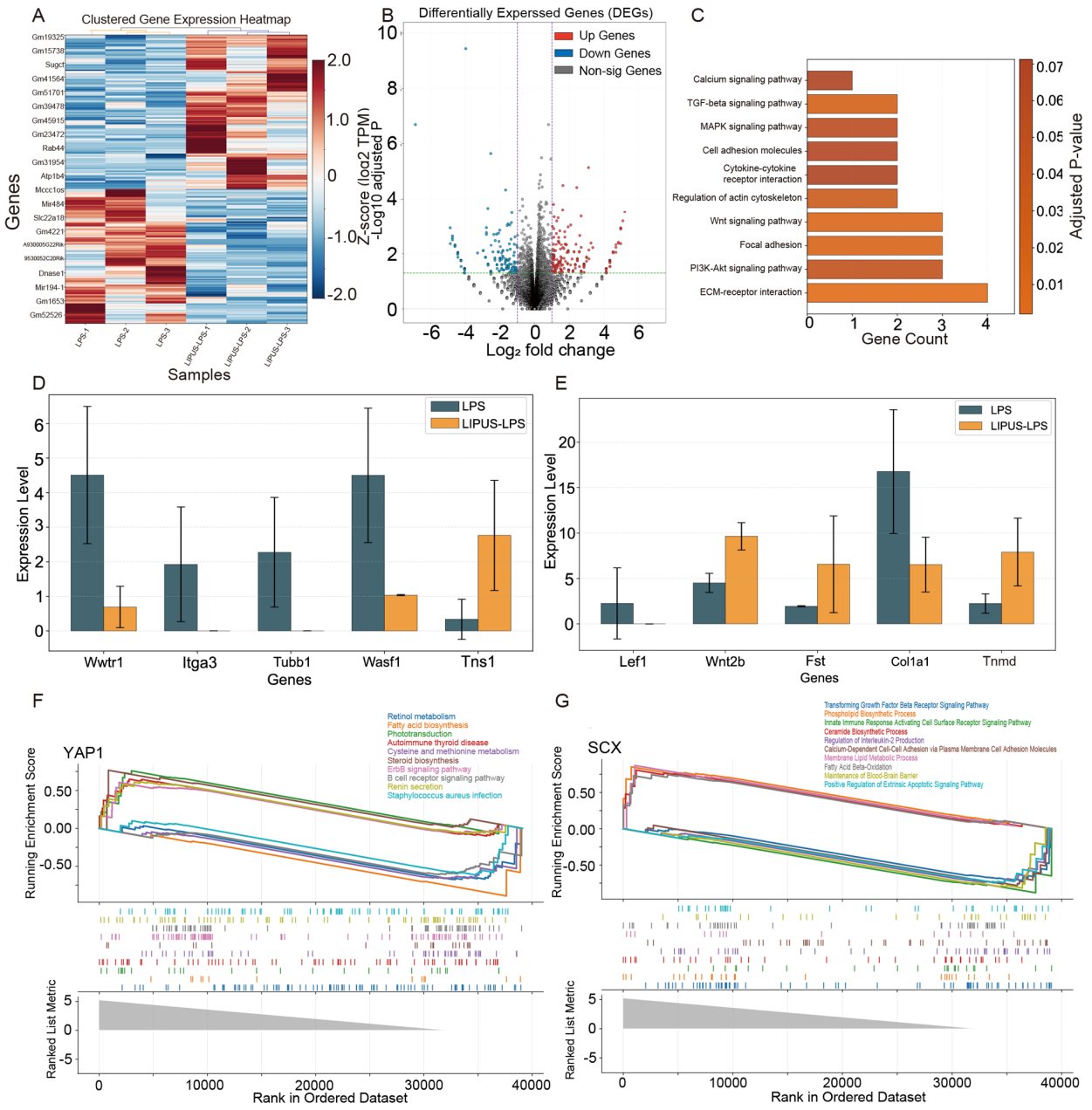

Figure 1. Transcriptomic profiling indicates that LIPUS activates mechanotransduction-related programs and enriches YAP/TAZ- and SCX-associated signatures in tendon stem cells. (A) Heatmap showing the global expression pattern of DEGs between the Control and LIPUS groups. (B) Volcano plot showing significantly upregulated and downregulated genes after LIPUS stimulation. (C) Gene Ontology enrichment analysis of representative DEGs, highlighting biological processes related to mechanotransduction, cytoskeletal remodeling and structural adaptation. (D and E) RNA-sequencing-based expression profiles of representative mechano-sensing-related and tendon-associated transcripts selected from the differential expression analysis. (F and G) Gene set enrichment analysis demonstrating enrichment of YAP1- and SCX-related transcriptional signatures in the LIPUS group. Data are presented as the mean ± SD. LIPUS, low-intensity pulsed ultrasound; SCX, scleraxis; DEGs, differentially expressed genes.

predominantly associated with mechanotransduction-related processes, cytoskeletal organization and structural adaptation (Fig. 1C).

Representative RNA-seq results further indicated altered expression of selected mechano-sensing-related and tendon-associated transcripts after LIPUS exposure (Fig. 1D and E). In parallel, GSEA demonstrated significant enrichment of YAP1- and SCX-related signatures in the LIPUS group (Fig. 1F and G). Taken together, these data support the view that LIPUS induces a transcriptional program consistent with enhanced mechanotransduction and activation of tenogenesis-associated pathways.

Primary rat TSCs are successfully identified, and LIPUS enhances their migratory capacity. Primary cells isolated from rat Achilles tendon adhered readily to the culture surface and, after expansion, displayed a uniform spindle-shaped, fibroblast-like morphology characteristic of TSCs (Fig. 2A). Flow cytometric analysis showed that the cultured cells were strongly positive for CD90, CD105 and CD146. By contrast, only small fractions of cells were positive for the hematopoietic/inflammatory markers CD11b (5.65%) and CD45 (2.34%), while CD34 expression was also low (Fig. 2B). Thus, the overwhelming majority of cultured cells displayed the expected TSC-associated immunophenotypic profile,

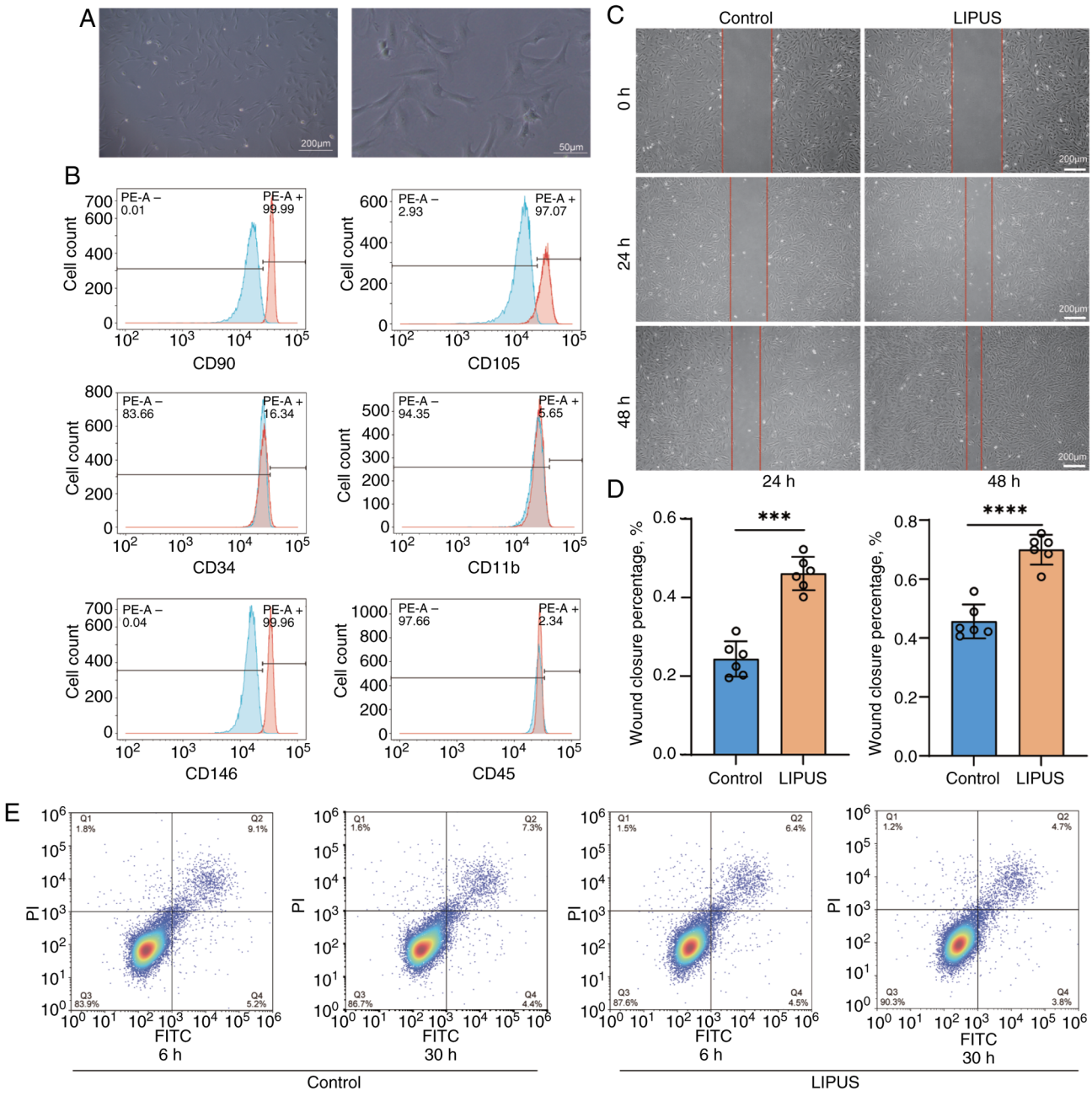

Figure 2. Characterization of primary rat TCSs, and the pro-migratory effect of LIPUS. For the LIPUS-treated samples in panels C-E, cells were exposed to LIPUS at 1.5 MHz and 50 mW/cm², with a pulse repetition frequency of 1 kHz and a 20% duty cycle, for 25 min per session on two occasions separated by 24 h. (A) Representative microscopic images of primary rat TSCs at low and high magnification, showing a spindle-shaped, fibroblast-like morphology. (B) Flow cytometric analysis of surface markers in cultured TSCs. Cells showed high expression of CD90, CD105 and CD146, whereas only minor fractions were positive for CD11b (5.65%) and CD45 (2.34%), supporting enrichment of a TSC-associated cell population. (C) Scratch-wound assay showing that LIPUS accelerated wound closure at 24 and 48 h compared with the Control group, with corresponding quantitative analysis of closure percentage (D). (E) Flow cytometric analysis of apoptosis using Annexin V-FITC/PI staining after LIPUS treatment. Representative plots showing apoptotic cell populations in the Control and LIPUS groups. Data are presented as the mean ± SD. ***P<0.001 and ****P<0.0001 vs. Control. TCSs, tendon stem cells; LIPUS, low-intensity pulsed ultrasound.

supporting successful enrichment of a stem/progenitor-like tendon-derived cell population with minimal hematopoietic contamination.

It was then examined whether LIPUS affected TSC migratory behavior using a scratch assay. Baseline wound widths were comparable between groups. At both 24 and 48 h, the LIPUS group showed a greater reduction in scratch area than the Control group, and quantitative analysis confirmed significantly increased scratch closure after LIPUS treatment (Fig. 2C and D). These findings indicate that LIPUS enhances the migratory activity of TSCs *in vitro*. Cell apoptosis was assessed by Annexin V-FITC/PI double staining and flow cytometry. As shown in Fig. E, compared with the Control group, LIPUS treatment did not increase apoptosis. The total apoptotic rate decreased from 14.3 and 11.7% to 10.9 and 8.5% at 6 and 30 h, respectively, indicating that LIPUS treatment exhibited favorable cytocompatibility without inducing obvious apoptosis.

LIPUS activates YAP/TAZ signaling and promotes tenogenic differentiation of TSCs. To determine whether LIPUS induced tenogenesis-associated molecular changes in TSCs, the expression of tendon-related markers was assessed together with key mechanotransduction mediators. Immunofluorescence staining showed that LIPUS markedly increased SCX and COL I expression relative to the Control group (Fig. 3A and B), and quantitative analysis confirmed significantly higher fluorescence intensities after LIPUS treatment (Fig. 3C and D).

At the transcriptional level, RT-qPCR demonstrated significant upregulation of Col I and Tnmd in the LIPUS group, supporting enhanced expression of matrix-related and tendon-associated genes. Western blot analysis further showed that LIPUS significantly increased the protein expression of YAP, TAZ and SCX (Fig. 3E and F). Collectively, these findings indicate that LIPUS activates YAP/TAZ-associated signaling and enhances a tenogenesis-associated molecular phenotype in TSCs. YAP subcellular localization was evaluated by immunofluorescence staining. Compared with the Control group, LIPUS treatment significantly increased the nuclear localization ratio of YAP, indicating enhanced YAP nuclear translocation and activation of YAP signaling (Fig. 3G and H).

Inhibition of YAP/TAZ suppresses LIPUS-induced tenogenic differentiation and matrix synthesis. To determine whether the effects of LIPUS were associated with YAP/TAZ signaling, pharmacological inhibition experiments were performed using VP. Immunofluorescence staining showed that the LIPUS-induced increases in SCX and COL I were markedly attenuated by VP treatment (Fig. 4A and B), and quantitative analysis confirmed a significant reduction in fluorescence intensity in the LIPUS + VP group (Fig. 4C and D).

Consistent with these findings, RT-qPCR showed that the LIPUS-induced upregulation of Col I and Tnmd was significantly suppressed by VP. Western blot analysis further demonstrated that VP reduced the expression of YAP, TAZ, SCX and COL I relative to LIPUS treatment alone (Fig. 4E and F). On the basis of these results, a working model was presented, in which LIPUS-derived mechanical cues activate YAP/TAZ-associated signaling, increase SCX expression, and thereby enhance tenogenesis-associated responses and matrix-related gene expression in TSCs (Fig. 4G).

Discussion

In the present study, LIPUS induced transcriptomic and molecular changes in rat TSCs that were consistent with activation of mechanotransduction and enhancement of a tenogenesis-associated program. By integrating bioinformatic analysis with *in vitro* experiments, it was found that LIPUS enriched pathways related to mechanical signaling and cytoskeletal remodeling, increased scratch closure, and upregulated YAP, TAZ, SCX, COL I and TNMD. Moreover, pharmacological inhibition with VP attenuated these effects, supporting the involvement of YAP/TAZ-associated signaling in the cellular response to LIPUS.

A key observation in the present study is that LIPUS reshaped the transcriptomic landscape of TSCs toward a mechanosensitive state. The enriched BP were primarily related to mechanotransduction and cytoskeletal organization, in line with the concept that stem cells convert physical cues into transcriptional outputs through membrane-associated mechano-sensors and actin-dependent signaling networks (25-28). This finding is mechanistically relevant because YAP/TAZ activity is tightly coupled to cytoskeletal tension, cell shape and cell-matrix interactions (13,14,29,30). The present transcriptomic data therefore provide a plausible upstream framework linking LIPUS-derived mechanical stimulation to downstream changes in tendon-associated gene regulation. Finally, the upstream mechanosensitive pathways linking LIPUS exposure to YAP/TAZ activation were not directly examined. Thus, although the present findings support the involvement of the YAP/TAZ/SCX axis, they do not establish the precise upstream molecular sequence. Further studies are required to define the roles of integrins, Piezo channels, calcium signaling and cytoskeletal remodeling in this process.

Because LIPUS may influence cytoskeletal signaling and YAP/TAZ activity, the suitability of β-actin as a loading control warrants consideration. Mechanical stimulation can alter actin filament organization, polymerization, intracellular tension and cell morphology; however, such changes do not necessarily indicate a change in total β-actin protein abundance. In the present study, β-actin bands showed no apparent differences among the Control, LIPUS and LIPUS + VP groups under the applied treatment conditions (50 mW/cm^2; two 25-min sessions separated by 24 h). Therefore, β-actin was used to normalize protein loading in the western blot analyses. This result should be interpreted as stability of total β-actin abundance under the specific conditions of the present study and does not exclude LIPUS-induced remodeling of the actin cytoskeleton.

It should be noted that primary tendon-derived cultures are intrinsically heterogeneous. Although CD11b and CD45 were used as negative markers for TSC characterization, low proportions of CD11b-positive (5.65%) and CD45-positive (2.34%) cells were detected in the present study. These minor populations may represent residual non-TSC cells after primary isolation or low-level background staining. Importantly, the predominant cell population was positive for CD90, CD105 and CD146 and negative for hematopoietic-associated markers overall. Therefore, TSC identification was based on the combined marker profile rather than on complete absence of each negative marker in every individual cell.

SCX is a central regulator of tendon development and maintenance of the tenogenic program (15,16,31,32). In the present study, SCX was increased after LIPUS treatment at the transcriptomic and/or targeted experimental levels, together with increased expression of COL I and TNMD in targeted assays. These findings support the interpretation that LIPUS enhances a tendon-associated molecular phenotype rather than merely altering a non-specific stress-response program. Because YAP/TAZ function as mechanosensitive transcriptional coactivators that regulate lineage-associated gene expression (33-39), the concurrent increase in YAP/TAZ and SCX is consistent with the involvement of a functional YAP/TAZ-SCX signaling axis in this process. Notably,

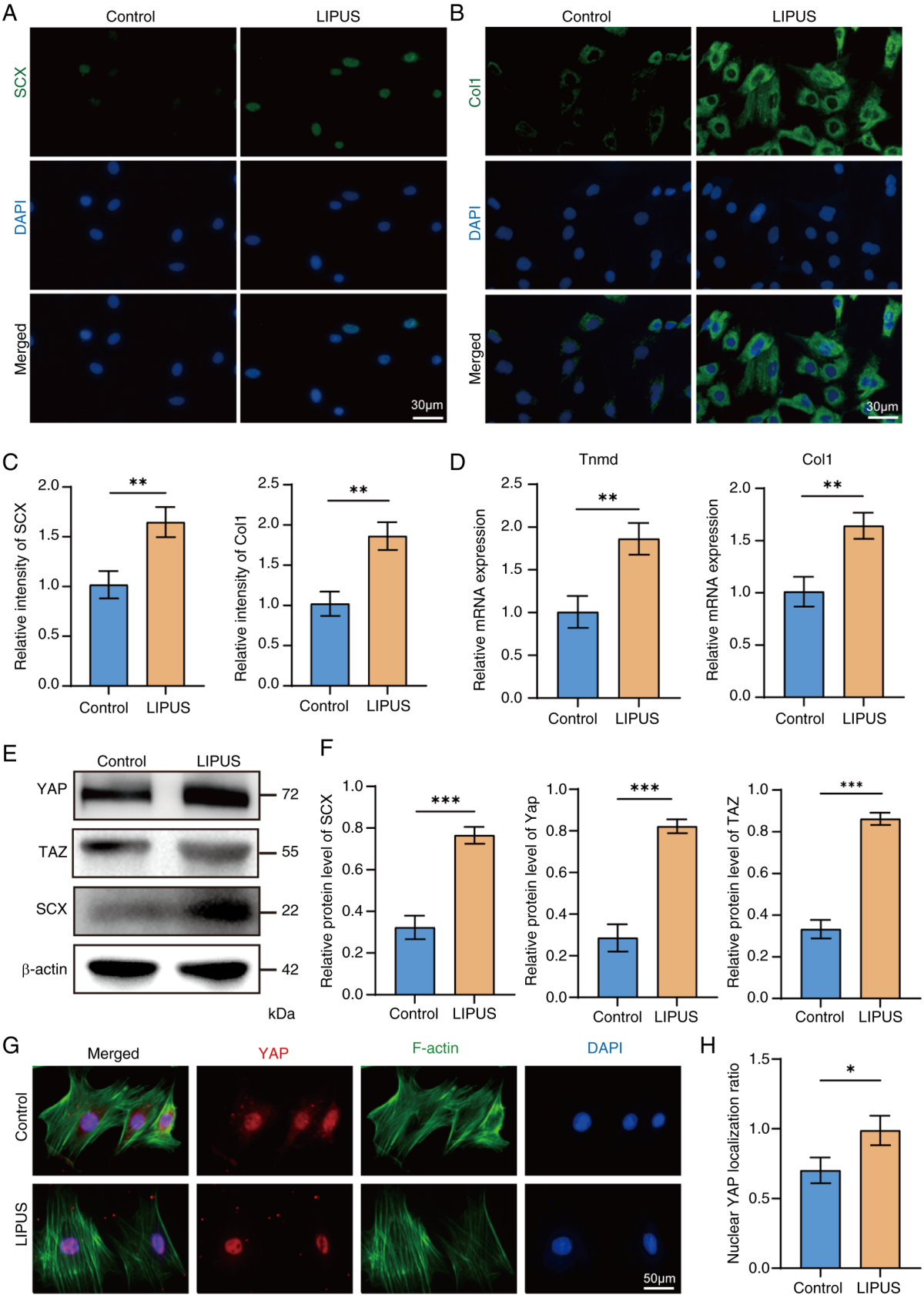

Figure 3. LIPUS enhances YAP/TAZ-associated signaling and increases tenogenesis-associated marker expression in tendon stem cells. TSCs in the LIPUS group were treated with LIPUS at 1.5 MHz and 50 mW/cm², with a pulse repetition frequency of 1 kHz and a 20% duty cycle, for two 25-min sessions separated by 24 h. (A and B) Representative immunofluorescence images showing increased SCX and COL I expression in TSCs after LIPUS treatment. (C and D) Quantitative analysis of immunofluorescence intensity together with reverse transcription-quantitative PCR analysis of tendon-associated markers, showing increased expression in the LIPUS group. (E and F) Western blot analysis and densitometric quantification demonstrating increased YAP, TAZ and SCX protein levels after LIPUS stimulation. Immunofluorescence analysis of YAP localization after LIPUS treatment. (G) Representative images of YAP (red), F-actin (green) and nuclei (DAPI, blue). (H) Quantification of nuclear YAP localization ratio. Data are presented as the mean ± SD. *P<0.05, **P<0.01 and ***P<0.001 vs. Control. LIPUS, low-intensity pulsed ultrasound; TCSs, tendon stem cell; SCX, scleraxis.

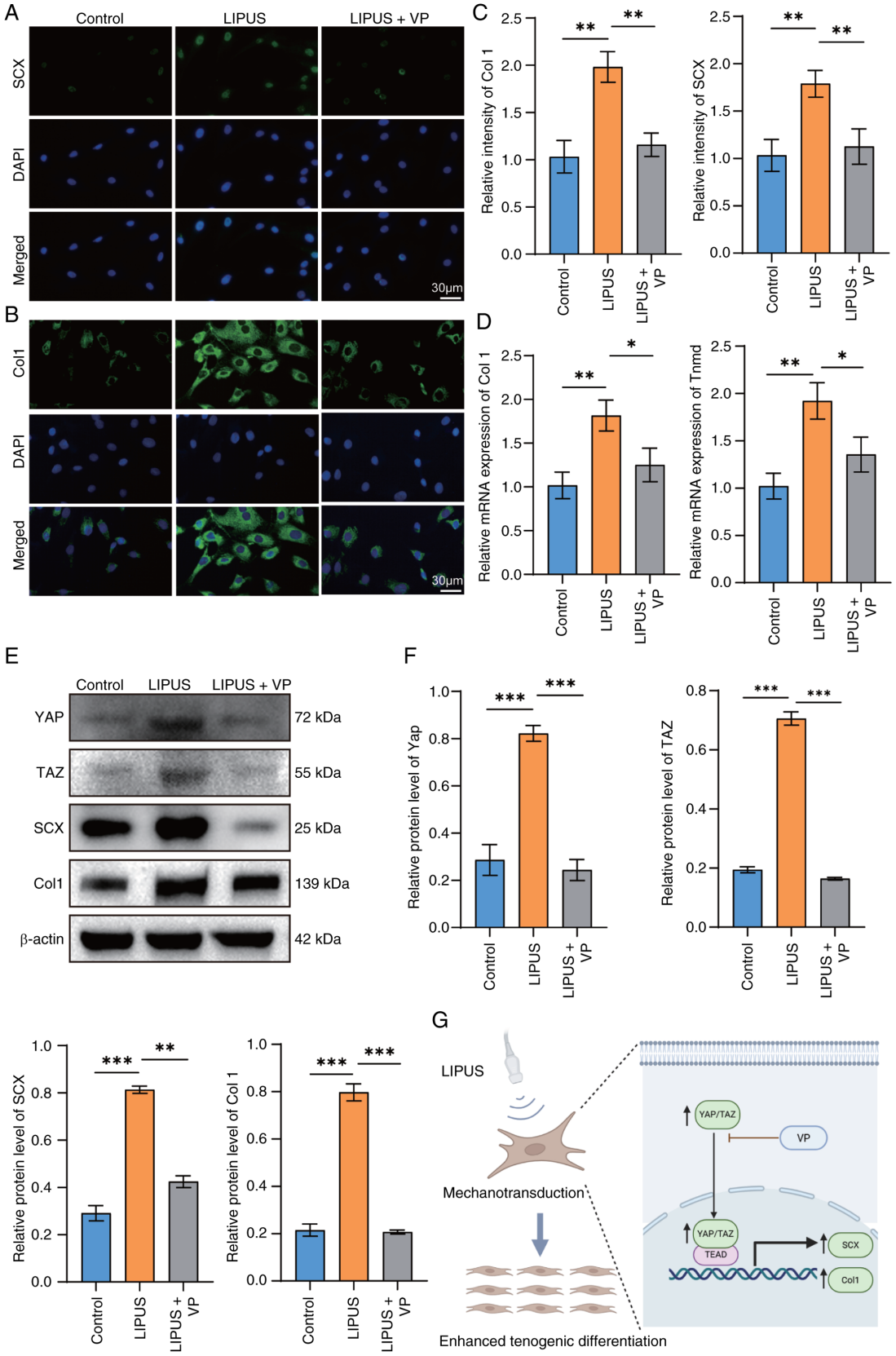

Figure 4. Pharmacological inhibition of YAP/TAZ attenuates LIPUS-induced tenogenesis-associated responses and matrix-related marker expression. TSCs in the LIPUS and LIPUS + VP groups received LIPUS at 1.5 MHz and 50 mW/cm^2, with a pulse repetition frequency of 1 kHz and a 20% duty cycle, for two 25-min sessions separated by 24 h. In the LIPUS + VP group, cells were pretreated with VP (1 μmol/l) for 1 h before each LIPUS session. (A and B) Representative immunofluorescence images of SCX and COL I in the Control, LIPUS and LIPUS + VP groups. (C and D) Quantitative immunofluorescence and reverse transcription-quantitative PCR analyses showing that VP reduced the LIPUS-induced increase in tendon-associated marker expression. (E and F) Western blot analysis and densitometric quantification demonstrating that VP suppressed the LIPUS-mediated increase in YAP, TAZ, SCX and COL I protein expression. (G) Proposed working model illustrating that LIPUS enhances tenogenesis-associated responses in TSCs through mechanotransduction-dependent activation of YAP/TAZ-associated signaling and upregulation of SCX. Data are presented as the mean ± SD. *P<0.05, **P<0.01 and ***P<0.001. LIPUS, low-intensity pulsed ultrasound; TCSs, tendon stem cell; VP, Verteporfin.

COL I and TNMD were validated primarily by targeted assays rather than emphasized in the RNA-seq display, which most likely reflects differences in transcript selection, analytical thresholds and figure presentation rather than a true biological inconsistency.

The inhibitor experiments using VP further strengthened this interpretation. VP attenuated the LIPUS-induced increases in YAP, TAZ, SCX, COL I, and TNMD, indicating that YAP/TAZ activity contributes materially to the downstream molecular response. This observation is biologically plausible because YAP/TAZ signaling interacts with other developmental pathways, including TGF-β and Wnt, to regulate cell fate decisions (37,38,40-45). Although these pathways were not directly interrogated in the present study, the current findings position YAP/TAZ as an important signaling node through which mechanical stimulation may be integrated with broader regulatory networks during tendon repair.

Another notable finding is that LIPUS enhanced TSC migratory behavior *in vitro*. Efficient cell migration is relevant to tendon repair because progenitor cells must populate the injury site before participating in tissue remodeling. In this context, the increased scratch closure observed after LIPUS exposure suggests improved migratory capacity rather than accelerated tissue healing per se, and the wording should therefore be interpreted accordingly.

Several limitations should be acknowledged. First, the current data support enhancement of a tenogenesis-associated molecular phenotype, but they do not by themselves establish complete tenocyte maturation. Second, the study was performed entirely *in vitro* and therefore cannot fully recapitulate the biomechanical, inflammatory, vascular and extracellular matrix microenvironment of injured tendon tissue *in vivo*. Thus, the observed effects of LIPUS should not be directly extrapolated to functional tendon healing outcomes. Future studies using rat or mouse Achilles tendon injury models will be required to evaluate histological repair, collagen organization, biomechanical strength and *in vivo* activation of the YAP/TAZ/SCX axis. Third, the transcriptomic analysis was based on an external LIPUS-related dataset rather than the current TSC model, which may introduce system-dependent differences. Therefore, these findings should be considered supportive evidence and require further validation in LIPUS-treated TSCs. Finally, additional lineage markers, functional assays and *in vivo* validation will be needed to strengthen causal inference and clarify the hierarchical relationship between YAP/TAZ, SCX, and other mechanosensitive pathways.

Furthermore, TSCs in the present study were derived from 3-4-week-old male rats; thus, variability associated with donor age, sex, individual donors and cell batches was not systematically evaluated. Future studies should include multiple donors of different ages and sexes to improve the generalizability of the findings. In addition, neither a VP-only group nor a vehicle-control group was included. Although no overt morphological abnormalities or cytotoxicity were observed under the treatment conditions, potential off-target effects of VP cannot be completely excluded. Future investigations should therefore incorporate appropriate pharmacological controls and complementary genetic approaches, such as YAP/TAZ knockdown, to further confirm pathway specificity.

Taken together, these findings indicate that LIPUS is not merely a passive physical adjunct, but a biologically active modulator of TSC behavior. By engaging mechanotransduction-related signaling, particularly the YAP/TAZ/SCX axis, LIPUS may represent a promising noninvasive approach for the enhancement of tendon regeneration.

In conclusion, LIPUS enhances tenogenesis-associated molecular responses and matrix-related marker expression in rat TSCs. Mechanistically, LIPUS activates mechanotransduction-related signaling, increases YAP/TAZ-associated activity, upregulates SCX, and elevates the expression of COL I and TNMD. Pharmacological inhibition with VP attenuates these effects, indicating that the cellular response to LIPUS is closely associated with activation of the YAP/TAZ/SCX axis. These findings provide a mechanistic rationale for further evaluation of LIPUS in tendon regeneration.

Acknowledgements

Not applicable.

Funding

The present study was supported by the Open Fund of the Hubei Key Laboratory of Tumor Microenvironment and Immunotherapy, China Three Gorges University (grant no. 2024KZL010).

Availability of data and materials

The data generated in the present study may be requested from the corresponding author.

Authors' contributions

SL and YL conceived and designed the study. SL and YH contributed to methodology design and performed data analysis using software. KZ, LC and DL conducted formal analysis. YL was responsible for data curation and investigation. SL and DL wrote the original draft. All authors reviewed and critically revised the manuscript, approved the final version of the manuscript, and agreed to be accountable for all aspects of the work. SL and YL confirm the authenticity of all the raw data.

Ethics approval and consent to participate

The present study was approved by the Animal Welfare Ethics Committee of the Second Hospital of Shanxi Medical University (approval no. DW20230008; Taiyuan, China), and all procedures were conducted in accordance with institutional and national guidelines for animal care and use.

Patient consent for publication

Not applicable.

Competing interests

The authors declare that they have no competing interests.

References

1. Ellis I, Schnabel LV and Berglund AK: Defining the profile: Characterizing cytokines in tendon injury to improve clinical therapy. J Immunol Regen Med 16: 100059, 2022.
2. Malik SS, Tahir M and D'Alessandro P: Tendon injuries. In: Textbook of Musculoskeletal Disorders. Longo UG and Denaro V (eds). Springer International Publishing, Cham, pp461-466, 2023.
3. Yoshimoto Y and Oishi Y: Mechanisms of skeletal muscle-tendon development and regeneration/healing as potential therapeutic targets. Pharmacol Ther 243: 108357, 2023.
4. Dyment NA and Galloway JL: Regenerative biology of tendon: Mechanisms for renewal and repair. Curr Mol Biol Rep 1: 124-131, 2015.
5. Łuczak JW, Palusińska M, Matak D, Pietrzak D, Nakielski P, Lewicki S, Grodzik M and Szymański Ł: The future of bone repair: Emerging technologies and biomaterials in bone regeneration. Int J Mol Sci 25: 12766, 2024.
6. Abyzova E, Dogadina E, Rodriguez RD, Petrov I, Kolesnikova Y, Zhou M, Liu C and Sheremet E: Beyond tissue replacement: The emerging role of smart implants in healthcare. Mater Today Bio 22: 100784, 2023.
7. Fennell N and Tucker S: Principles of tendon repair. Surgery (Oxford) 34: 152-156, 2016.
8. Zhang X, Zhang S and Wang T: How the mechanical microenvironment of stem cell growth affects their differentiation: A review. Stem Cell Res Ther 13: 415, 2022.
9. Han SB, Kim JK, Lee G and Kim DH: Mechanical properties of materials for stem cell differentiation. Adv Biosyst 4: 2000247, 2020.
10. Long Y, Wang P, Lei J, Su B, Wei Q and Liu X: Mechanical signaling: Molecular mechanisms, biological functions, diseases, and therapeutic targets. MedComm (2020) 6: e70523, 2025.
11. Xie N, Xiao C, Shu Q, Cheng B, Wang Z, Xue R, Wen Z, Wang J, Shi H, Fan D, *et al*: Cell response to mechanical microenvironment cues via Rho signaling: From mechanobiology to mechanomedicine. Acta Biomater 159: 1-20, 2023.
12. Liu Z, Chen G, Jo MS, Vogel V, Chen J, Rogers JA and Li S: Mechanomedicine. Nat Rev Bioeng 4: 216-235, 2026.
13. Hansen CG, Moroishi T and Guan KL: YAP and TAZ: A nexus for Hippo signaling and beyond. Trends Cell Biol 25: 499-513, 2015.
14. Totaro A, Panciera T and Piccolo S: YAP/TAZ upstream signals and downstream responses. Nat Cell Biol 20: 888-899, 2018.
15. Paterson YZ, Evans N, Kan S, Cribbs A, Henson FMD and Guest DJ: The transcription factor scleraxis differentially regulates gene expression in tenocytes isolated at different developmental stages. Mech Dev 163: 103635, 2020.
16. Sakabe T, Sakai K, Maeda T, Sunaga A, Furuta N, Schweitzer R, Sasaki T and Sakai T: Transcription factor scleraxis vitally contributes to progenitor lineage direction in wound healing of adult tendon in mice. J Biol Chem 293: 5766-5780, 2018.
17. Liang W, Liang B, Yan K, Zhang G, Zhuo J and Cai Y: Low-intensity pulsed ultrasound: A physical stimulus with immunomodulatory and anti-inflammatory potential. Ann Biomed Eng 52: 1955-1981, 2024.
18. Berber R, Aziz S, Simkins J, Lin SS and Mangwani J: Low intensity pulsed ultrasound therapy (LIPUS): A review of evidence and potential applications in diabetics. J Clin Orthop Trauma 11 (Suppl 4): S500-S505, 2020.
19. Wang Q, Zeng X, Yang H, Lu H, Jiang L, Xu L, Li J, Li J, Han Y, Wu X, *et al*: Transient mechanical activation of the Piezo1 channel facilitates ex vivo expansion of hematopoietic stem cells. Cell Res 36: 272-285, 2026.
20. Raman N, Imran SAM, Ahmad Amin Noordin KB, Zaman WSWK and Nordin F: Mechanotransduction in mesenchymal stem cells (MSCs) differentiation: A review. Int J Mol Sci 23: 4580, 2022.
21. Lai WC, Iglesias BC, Mark BJ and Wang D: Low-intensity pulsed ultrasound augments tendon, ligament, and bone-soft tissue healing in preclinical animal models: A systematic review. Arthroscopy 37: 2318-2333.e3, 2021.
22. Li S, Xu Z, Wang Z, Xiang J, Zhang T and Lu H: Acceleration of bone-tendon interface healing by low-intensity pulsed ultrasound is mediated by macrophages. Phys Ther 101: pzab055, 2021.
23. Livak KJ and Schmittgen TD: Analysis of relative gene expression data using real-time quantitative PCR and the 2(-Delta Delta C(T)) method. Methods 25: 402-408, 2001.
24. Yin J, Bao Y, Xu M, Li P, Zhang Z, Xue H and Yang X: Anti-inflammatory role of low-intensity pulsed ultrasound in inhibiting lipopolysaccharide-induced M1 polarization of RAW264.7 cells via Wnt2b/AXIN/β-catenin. PeerJ 12: e18448, 2024.
25. Udroiu I, Todaro F, Vitaliti A, Palmieri D, Guida E, Perilli G, Duranti L, D'Ottavi C, Mattei M, Dolci S, *et al*: Low-intensity pulsed ultrasound induces multifaced alterations in chromosome segregation, cytoskeletal filaments and cell junctions. Sci Rep 15: 4964, 2025.
26. Li X, Zhong Y, Zhang L and Xie M: Recent advances in the molecular mechanisms of low-intensity pulsed ultrasound against inflammation. J Mol Med (Berl) 101: 361-374, 2023.
27. Lu J, Chen H, Lyu K, Jiang L, Chen Y, Long L, Wang X, Shi H and Li S: The functions and mechanisms of tendon stem/progenitor cells in tendon healing. Stem Cells Int 2023: 1258024, 2023.
28. Xia P, Shi Y, Wang X and Li X: Advances in the application of low-intensity pulsed ultrasound to mesenchymal stem cells. Stem Cell Res Ther 13: 214, 2022.
29. Chen X, Ji X, Lao Z, Pan B, Qian Y and Yang W: Role of YAP/TAZ in bone diseases: A transductor from mechanics to biology. J Orthop Translat 51: 13-23, 2025.
30. Zarka M, Haÿ E and Cohen-Solal M: YAP/TAZ in bone and cartilage biology. Front Cell Dev Biol 9: 788773, 2022.
31. Huang AH, Lu HH and Schweitzer R: Molecular regulation of tendon cell fate during development. J Orthop Res 33: 800-812, 2015.
32. Havis E, Bonnin MA, Esteves de Lima J, Charvet B, Milet C and Duprez D: TGFβ and FGF promote tendon progenitor fate and act downstream of muscle contraction to regulate tendon differentiation during chick limb development. Development 143: 3839-3851, 2016.
33. Wei Y, Hui VLZ, Chen Y, Han R, Han X and Guo Y: YAP/TAZ: Molecular pathway and disease therapy. MedComm (2020) 4: e340, 2023.
34. Battilana G, Zanconato F and Piccolo S: Mechanisms of YAP/TAZ transcriptional control. Cell Stress 5: 167-172, 2021.
35. Pocaterra A, Romani P and Dupont S: YAP/TAZ functions and their regulation at a glance. J Cell Sci 133: jcs230425, 2020.
36. Sato K, Faraji F, Cervantes-Villagrana RD, Wu X, Koshizuka K, Ishikawa T, Iglesias-Bartolome R, Chen L, Miliani de Marval PL, Gwaltney SL, *et al*: Targeting YAP/TAZ-TEAD signaling as a therapeutic approach in head and neck squamous cell carcinoma. Cancer Lett 612: 217467, 2025.
37. Ajongbolo AO and Langhans SA: YAP/TAZ-associated cell signaling-at the crossroads of cancer and neurodevelopmental disorders. Front Cell Dev Biol 13: 1522705, 2025.
38. Heng BC, Zhang X, Aubel D, Bai Y, Li X, Wei Y, Fussenegger M and Deng X: An overview of signaling pathways regulating YAP/TAZ activity. Cell Mol Life Sci 78: 497-512, 2021.
39. Jafarinia H, Khalilimeybodi A, Barrasa-Fano J, Fraley SI, Rangamani P and Carlier A: Insights gained from computational modeling of YAP/TAZ signaling for cellular mechanotransduction. NPJ Syst Biol Appl 10: 90, 2024.
40. Qin Z, Xia W, Fisher GJ, Voorhees JJ and Quan T: YAP/TAZ regulates TGF-β/Smad3 signaling by induction of Smad7 via AP-1 in human skin dermal fibroblasts. Cell Commun Signal 16: 18, 2018.
41. Miranda MZ, Bialik JF, Speight P, Dan Q, Yeung T, Szászi K, Pedersen SF and Kapus A: TGF-β1 regulates the expression and transcriptional activity of TAZ protein via a Smad3-independent, myocardin-related transcription factor-mediated mechanism. J Biol Chem 292: 14902-14920, 2017.
42. Xue C, Chu Q, Shi Q, Zeng Y, Lu J and Li L: Wnt signaling pathways in biology and disease: Mechanisms and therapeutic advances. Signal Transduct Target Ther 10: 106, 2025.
43. Baarsma HA, Königshoff M and Gosens R: The WNT signaling pathway from ligand secretion to gene transcription: Molecular mechanisms and pharmacological targets. Pharmacol Ther 138: 66-83, 2013.
44. Wu S, Zhou H, Ling H, Sun Y, Luo Z, Ngo T, Fu Y, Wang W and Kong Y: LIPUS regulates the progression of knee osteoarthritis in mice through primary cilia-mediated TRPV4 channels. Apoptosis 29: 785-798, 2024.
45. Heng BC, Zhang X, Aubel D, Bai Y, Li X, Wei Y, Fussenegger M and Deng X: Role of YAP/TAZ in cell lineage fate determination and related signaling pathways. Front Cell Dev Biol 8: 735, 2020.